

Phase-Separation Kinetics in Protein–Salt Mixtures with Compositionally Tuned Interactions

Olga Matsarskaia,^{*,†} Stefano Da Vela,^{†,||} Alessandro Mariani,^{‡,⊥} Zhendong Fu,^{§,#} Fajun Zhang,[†] and Frank Schreiber^{*,†}

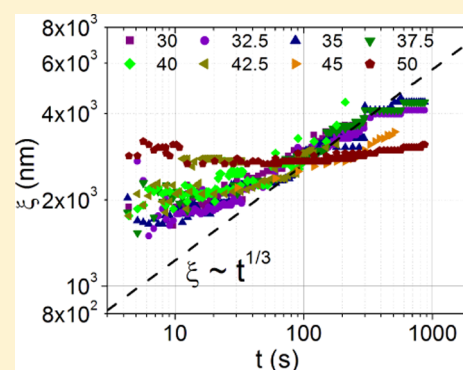
[†]Institut für Angewandte Physik, Universität Tübingen, Auf der Morgenstelle 10, 72076 Tübingen, Germany

[‡]European Synchrotron Radiation Facility, 71 Avenue des Martyrs, 38043 Grenoble Cedex 9, France

[§]Forschungszentrum Jülich GmbH, JCNS@MLZ, Lichtenbergstrasse 1, 85747 Garching, Germany

Supporting Information

ABSTRACT: Liquid–liquid phase separation (LLPS) in protein systems is relevant for many phenomena, from protein condensation diseases to subcellular organization to possible pathways toward protein crystallization. Understanding and controlling LLPS in proteins is therefore highly relevant for various areas of (biological) soft matter research. Solutions of the protein bovine serum albumin (BSA) have been shown to have a lower critical solution temperature–LLPS (LCST–LLPS) inducible by multivalent salts. Importantly, the nature of the multivalent cation used influences the LCST–LLPS in such systems. Here, we present a systematic ultrasmall-angle X-ray scattering investigation of the kinetics of LCST–LLPS of BSA in the presence of different mixtures of HoCl_3 and LaCl_3 , resulting in different effective interprotein attraction strengths. We monitor the characteristic length scales $\xi(t, T_{\text{fin}})$ after inducing LLPS by subjecting the respective systems to temperature jumps in their liquid–liquid coexistence regions. With increasing interprotein attraction and increasing T_{fin} , we observe an increasing deviation from the growth law of $\xi \sim t^{1/3}$ and an increased trend toward arrest. We thus establish a multidimensional method to tune phase transitions in our systems. Our findings help shed light on general questions regarding LLPS and the tunability of its kinetics in both proteins and colloidal systems.



INTRODUCTION

Liquid–liquid phase separation (LLPS) is known to occur in a variety of systems from mixtures of organic molecules to colloidal matter with, in many cases, complex interaction potentials. When occurring in protein systems, metastable LLPS plays an important role in cellular organization, signaling, and development.^{1–5} Furthermore, LLPS is related to the main reason behind protein condensation diseases such as cataract⁶ and sickle cell anemia⁷ and can influence the properties of protein-based therapeutics.^{8–10} In addition, several properties of industrial food products are similarly governed by phase separation phenomena.^{11,12} Importantly, the density inhomogeneity associated with LLPS can be an important precursor for protein crystallization.^{13–15} Understanding and rationally manipulating LLPS in protein solutions is thus of strong interest for several areas of biological and soft matter research.

The two main mechanisms leading to liquid–liquid phase separation are nucleation and spinodal decomposition (SD), which take place in the metastable and unstable regions of the area inside the binodal of the phase diagram of the system in question. Nucleation is often described via classical nucleation theory (see, e.g., ref 16), whereas SD is commonly rationalized using the Cahn–Hilliard theory relating the temporal variation of concentration fluctuations $\frac{\partial \delta c(r,t)}{\partial t}$ to the changes in the free

energy F of the system.^{16–19} In the late stages of SD, coarsening according to Lifshitz and Slyozov^{16,20,21} and Binder and Stauffer²² predicts a time-dependent growth of the characteristic length ξ of the respective system according to the power law $\xi \sim t^{1/3}$.

LLPS, SD, and their interplays with phenomena such as arrested phase transitions have been studied both theoretically and experimentally in a variety of systems such as metal alloys^{23,24} and polymer blends,^{25,26} as well as colloidal systems (see, e.g., refs 27–32 and 33 for a review).

It was found experimentally and established theoretically^{34–38} that a metastable LLPS in colloidal systems can be traced back to short-ranged (i.e., much smaller than the particle diameter³⁷) attractions between the colloids. Importantly, this concept established in colloid science is, within certain approximations and limits, applicable to many protein systems, since the latter typically also exhibit short-ranged interparticle attraction.³⁹ Under certain conditions, protein systems can also undergo a metastable LLPS,^{40–50} which can

Received: November 3, 2018

Revised: January 10, 2019

Published: January 31, 2019

be described and rationalized using concepts from colloid theory.

For example, Shah et al.⁴⁶ observed a continuous transition from metastable to unstable phase separation mechanisms in aqueous lysozyme solutions with an upper critical solution temperature (UCST) for varying temperature quench depths. A further experimental study on lysozyme by Cardinaux et al.⁴⁷ reported that the quench depth into the coexisting region determines whether the system undergoes complete LLPS or whether glass formation interferes with the latter. These results were later confirmed by Gibaud et al.,⁴⁹ who showed that the arrested two-phase system obtained by Cardinaux et al.⁴⁷ consisted of a bicontinuous network in an arrested state. The work by Gibaud et al.⁴⁹ also clearly illustrates the change of the growth exponent α of $\xi \sim t^\alpha$ with increasing time. Although α is equal to 1/3 in the initial stages of growth, there is a substantial slowing down in the late stages of the experiment, i.e., for large t . The network obtained for deep quenches is the result of an arresting spinodal decomposition in the early stages of critical quenches.

Throughout the past years, our group has established a model system of proteins in aqueous solutions with a short-range interprotein attraction induced by multivalent cations.^{14,51–65} Among other phenomena, this short-range attraction leads to a metastable LLPS,^{53,56} which can play an active role in the nucleation and growth of protein crystals.^{14,53,55,59,60} The short-range interprotein attraction induced by multivalent cations has been rationalized by a cation-activated patchy particle model.^{66,67} Binding patches on the surface of proteins are known not only for ions but also for more complex ligands such as pharmaceuticals.⁶⁸ Notably, the LLPS in our systems is entropically driven and appears as temperature increases, i.e., it features a lower critical solution temperature (LCST–LLPS).^{62–64} A recent study reported that the type of multivalent cation used has a strong influence on the phase behavior on the LCST–LLPS of bovine serum albumin (BSA).⁶⁹ We established that using HoCl_3 induces strong a interprotein attraction, whereas the attraction is relatively weak in the case of LaCl_3 . Importantly, phase transitions of BSA can be fine-tuned by using different ratios of weakly and strongly interacting multivalent salts at constant ionic strength,⁶⁹ as notably manifested in shifts of the transition temperatures of phase-separating samples.

Having established the equilibrium phase diagrams of systems consisting of BSA and multivalent cations, here we study the kinetics of LLPS of BSA in the presence of multivalent salts via ultrasmall-angle X-ray scattering (USAXS), an experimental approach recently demonstrated in refs 64 and 70.

In particular, the present study focuses on the intriguing possibility of rationally manipulating the kinetics of phase separation in BSA-multivalent salt systems by changing their salt composition. Importantly, the control of the phase behavior of soft matter systems such as protein solutions opens up pathways toward controlled induction and tuning of different system properties such as phase separation and associated density fluctuations. The latter have been shown to facilitate the growth of protein crystals,¹³ which has crucial implications for crystallography and structural biology. In addition, the manipulation of stimulus-responsive systems is of fundamental interest for the design of the so-called smart materials⁷¹ or drug delivery systems.⁷² Establishing the role different factors play in controlling the phase behavior of soft

matter is therefore of fundamental importance in a variety of research areas. In the systems described in the present study, we use different ratios of the two multivalent salts HoCl_3 and LaCl_3 introducing strong and relatively weak interprotein attractions, respectively, to rationally tune the phase behavior of our systems. We find that with increasing HoCl_3 concentration, i.e., increasingly attractive protein interactions, the deviation from the $\xi \sim t^{1/3}$ growth law becomes pronounced and allows the experimental systems to enter an arrested state even in the case of small temperature jumps.

Exploiting the dependence our systems have on both the type of multivalent cation used and temperature, we thus establish a framework suitable for a multidimensional control of phase transitions of experimental systems. Our results are of general interest to areas of science concerned with fundamental research on phase separation thermodynamics and their mechanisms in colloids and proteins, and how these are affected by changes in microscopic interactions.

■ EXPERIMENTAL METHODS

Determination of Coexistence Regions of BSA– HoCl_3 / LaCl_3 Mixtures. Binodals reflecting the liquid–liquid coexistence regions of all samples were determined as follows. Samples containing initial protein concentrations of 175 mg/mL BSA and a total salt concentration of 40 mM consisting of HoCl_3 and LaCl_3 with the ratios 22/18, 25/15, and 30/10 mM were prepared in a water bath at temperatures from 12 to 45 °C by mixing appropriate amounts of protein and salt stock solutions. The samples were left to equilibrate for 20 min and subsequently centrifuged for 2 min at 21 000 rcf (Mikro 220R centrifuge, Hettich, Tuttlingen, Germany) at preparation temperature to facilitate separation into dense and dilute phases. The samples were equilibrated for 15 more minutes in the water bath at preparation temperature again, after which the volumes of both dense and dilute phases were determined by pipetting. The BSA concentrations of the dilute phases were measured by UV absorbance at $\lambda = 280$ nm.⁷³ The concentrations of the corresponding dense phases were calculated based on mass conservation.

USAXS Sample Preparation. BSA (catalogue number A7906, heat shock fraction) with a purity of $\geq 98\%$, as well as HoCl_3 (catalogue number 450901) and LaCl_3 (449830) (the respective purities were indicated as 99.9–99.99%), were purchased from Sigma Aldrich (now Merck, Darmstadt, Germany) and used as received. Protein and salt stock solutions were prepared by dissolving appropriate amounts of respective chemicals in degassed ultrapure (18.2 M Ω) MilliQ water (Merck Millipore, Darmstadt, Germany). The protein concentration of the stock solution was then determined by UV absorbance at $\lambda = 280$ nm.⁷³

Samples containing initial concentrations of 175 mg/mL BSA and different HoCl_3 / LaCl_3 ratios were prepared by mixing appropriate amounts of protein and salt stock solutions at room temperature (21 °C). The samples were centrifuged for 2 min at 21 000 rcf to facilitate the macroscopic separation of the dense and dilute phases. The samples were then stored at 21 °C overnight, after which the dilute phases were removed. The dense phases were stored at 5 °C for several hours until they became clear and were subsequently filled into quartz capillaries with a diameter of 1 mm using a syringe (Norm-Ject, Henke-Sass Wolf GmbH, Tuttlingen, Germany). Prolonged centrifugation at low speed and at 5 °C was then applied to remove air bubbles from the capillaries.

USAXS Measurements. The USAXS measurements were performed at beamline ID02^{74,75} (ESRF, Grenoble, France) using the 30 m sample detector distance setup. A $q = \frac{4\pi \sin \theta}{\lambda}$ range from 1.1×10^{-3} to $7.2 \times 10^{-2} \text{ nm}^{-1}$ was covered. The wavelength λ used was 0.995 \AA , corresponding to an energy of 12.46 keV . The signal was recorded using a FReLoN Kodak CCD detector.

Every measurement was performed by subjecting the respective sample to a temperature jump to a final temperature T_{fin} between 30 and $50 \text{ }^\circ\text{C}$ using a heating rate of 80 K/min . The starting temperature was $10 \text{ }^\circ\text{C}$. Throughout the experiment, the temperature was controlled using a temperature stage (Linkam Scientific Instruments, Surrey, U.K.). The USAXS measurements were divided into three distinct steps covering different stages of phase separation at the respective T_{fin} . In steps 1, 2, and 3, exposures were taken every 0.7 s , every 4 s , and every 30 s , respectively, as described in detail in ref ⁶⁴. At every step, the X-ray beam was focussed onto a different spot of the capillary to minimize radiation effects.⁶⁴ We note that the temperature jumps (i.e., heating) we use for our LCST systems correspond to the temperatures quenches (i.e., cooling) commonly described for colloidal and protein systems with a UCST (see, e.g., refs ⁴⁷ and ⁴⁹).

Prior to data analysis, the first featureless curve of each data set obtained at $10 \text{ }^\circ\text{C}$ before the temperature jump was subtracted from the following curves. The q value corresponding to the maximum intensity (q_{max}) was determined for each spectrum, and the characteristic length scale ξ was calculated as $\xi = 2\pi/q_{\text{max}}$.

Very Small-Angle Neutron Scattering (VSANS) Measurements. VSANS measurements were performed at beamline KWS-3 (FRM-II, Garching, Germany).⁷⁶ A $q = \frac{4\pi \sin \theta}{\lambda}$ range from 1.2×10^{-5} to $1.1 \times 10^{-3} \text{ \AA}^{-1}$ was covered. Samples with composition and preparation identical to those that used for USAXS measurements were filled into quartz cuvettes (type 404-QX, Hellma Optics, Jena, Germany) with a thickness of 1 mm and a total volume of 0.7 mL on ice and centrifuged extensively at $4 \text{ }^\circ\text{C}$ at very low speed (max. $20g$) to remove air bubbles. Prior to the measurement, the samples were kept on ice. To start the measurement, the samples were then placed onto a sample holder preheated to the desired T_{fin} via a circulating water bath (Julabo, Seelbach, Germany). VSANS profiles were recorded at intervals of $5\text{--}10 \text{ min}$ at respective T_{fin} for a total time of up to 2 h . Background correction was performed by subtracting the scattering profile of an empty sample cell. The correlation length ξ was calculated as $2\pi/q_{\text{max}}$.

RESULTS AND DISCUSSION

Binodals of BSA-HoCl₃/LaCl₃ Systems. To understand the influence different HoCl₃/LaCl₃ ratios have on the coexistence regions of the respective samples, the binodals of the samples with an initial BSA concentration of 175 mg/mL and varying initial salt ratios were measured by UV-vis spectroscopy. The binodals are displayed in Figure 1.

The binodals show a clear trend toward a higher difference in protein concentration (c_p) between dense and dilute phases with increasing HoCl₃ concentration, as indicated by the broadening of the coexistence regions with an increasing HoCl₃/LaCl₃ ratio. The samples used for the USAXS measurements (whose analysis is described below) are located

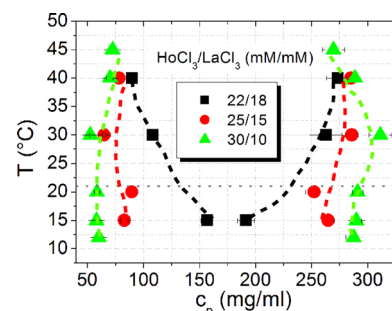


Figure 1. Binodals of corresponding dense and dilute phases obtained after LCST-LLPS of samples with $c_{p,\text{initial}} = 175 \text{ mg/mL}$ and varying initial salt ratios as shown in the legend. Dashed lines are guides to the eye. The gray dotted line indicates the preparation temperature of the samples. The samples used for the USAXS experiments described later on are located on the dense branches of the respective coexistences curves.

on the dense branch of the binodal. As seen in Figure 1, their protein concentrations (volume fractions) increase with increasing HoCl₃ concentration. The differences in phase behavior of the systems under investigation are therefore traced back to the salt composition itself, as well as to the salt composition-induced differences in their respective protein concentrations. This is discussed in more detail below.

In addition, the only sample composition in which an experimental approach toward the lower critical point above $0 \text{ }^\circ\text{C}$ is possible is the one with the lowest HoCl₃ concentration. A stronger overall interprotein attraction brought about by higher HoCl₃ concentrations presumably shifts the critical point toward lower temperatures, which cannot be reached within the temperature window accessible experimentally (i.e., above $0 \text{ }^\circ\text{C}$). This is consistent with cloud temperature data⁶⁹ where high HoCl₃ concentrations led to phase separation below the temperature window experimentally accessible.

Obtaining $\xi(t, T_{\text{fin}})$ from USAXS Profiles. A typical USAXS $I(q)$ plot obtained using a dense phase of an initial BSA concentration of 175 mg/mL and a HoCl₃/LaCl₃ ratio of $25/15$ ($T_{\text{fin}} = 45 \text{ }^\circ\text{C}$) is shown in Figure 2.

From the raw USAXS data, $\xi = 2\pi/q_{\text{max}}$ values were extracted and plotted as functions of time. Data sets of $\xi(t, T_{\text{fin}})$ for each sample composition and at different jumps to T_{fin} are shown in Figure 3.

In the case of the lowest HoCl₃ concentration (Figure 3a), $\xi(t, T)$ follows the power law growth of $\xi \sim t^{1/3}$ to a good approximation for all T_{fin} . Interestingly, the power law and its temperature dependence can be strongly influenced by different HoCl₃/LaCl₃ ratios as becomes apparent from a comparison of Figure 3a–c. With increasing T_{fin} and HoCl₃ concentration, the growth of $\xi(t, T_{\text{fin}})$ slows down, potentially approaching an apparently arrested state or strongly delayed kinetics of transformation at the highest T_{fin} and the highest concentrations of HoCl₃.

A possible scenario to rationalize the slowdown observed in the growth of ξ with increasing HoCl₃ concentrations would be as follows. First, a higher HoCl₃/LaCl₃ ratio widens the BSA-HoCl₃/LaCl₃ binodal and therefore influences the volume fraction of the USAXS samples that are located on the dense branch of the binodal (cf. Figure 1). In addition, multivalent salt has been shown to partition preferentially into the dense coexisting phase upon LLPS.⁵³ Moreover, the affinity of Ho³⁺ cations to BSA appears to be higher than that of La³⁺ cations.⁶⁹

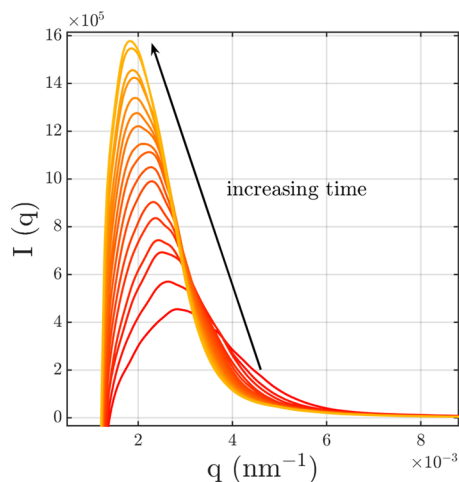


Figure 2. Typical raw USAXS data (initial BSA concentration = 175 mg/mL, $\text{HoCl}_3/\text{LaCl}_3$ ratio = 25/15, $T_{\text{fin}} = 45$ °C). Data were smoothed by binning every 5 points. The first curve corresponds to $t = 60$ s after the T jump, the last to $t = 510$ s. The characteristic length scale of the respective systems was calculated as $\xi = 2\pi/q_{\text{max}}$. The curves shown here were taken in time intervals of 30 s. See text for details.

Finally, Ho^{3+} cations induce a stronger interprotein attraction than La^{3+} cations.⁶⁹ It is therefore reasonable to assume that our samples are enriched with Ho^{3+} , which enhances the interprotein attraction. Thus, it seems likely that the combination of a higher protein volume fraction (which is more prone to arrest) and a stronger protein–protein attraction gives rise to the observed stronger tendency for arrest in the samples with more HoCl_3 and therefore deviates from the $\xi \sim t^{1/3}$ behavior.

We note that for systems with the highest HoCl_3 concentrations and the highest T_{fin} , the corresponding intensities $I(q_{\text{max}})$ feature a nonmonotonous behavior. In the present publication, however, we focus on the behavior of $\xi(t, T_{\text{fin}})$ and do not intend to analyze the behavior of the intensity. We note that although some of the samples appear kinetically hindered in some form for long observation times, we cannot rule out that under certain conditions, a slight coarsening of the structure might still occur for substantially longer times. Furthermore, we note that $\xi(t, T_{\text{fin}})$ saturates for very long time scales, as expected and as independently confirmed using very small-angle neutron scattering (VSANS)^{70,76} (see the Supporting Information).

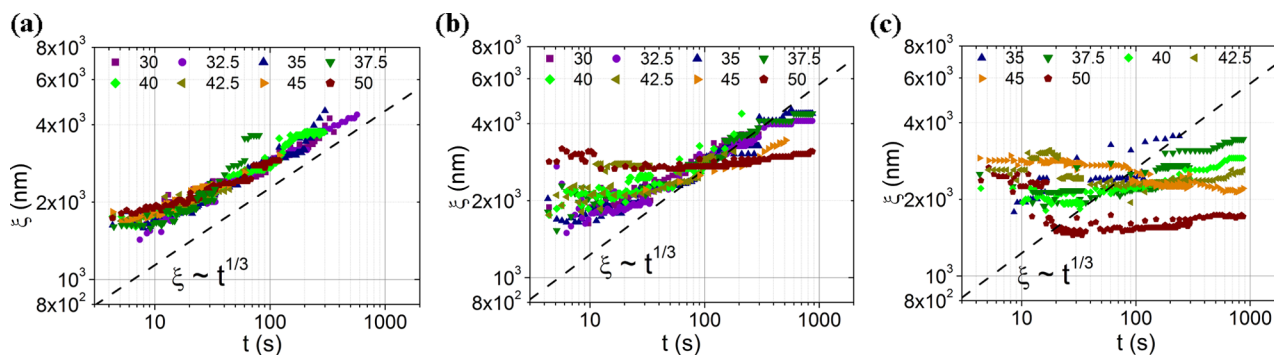


Figure 3. $\xi(t, T_{\text{fin}})$ profiles of different $\text{HoCl}_3/\text{LaCl}_3$ mixing ratios. The legends indicate T_{fin} (°C). We note that for long observation times t , $\xi(t, T_{\text{fin}})$ reaches a plateau as confirmed by very small-angle neutron scattering data (see the Supporting Information).

Interestingly, the plateau value of $\xi(t, T_{\text{fin}})$ in the samples containing the highest $\text{HoCl}_3/\text{LaCl}_3$ ratio shows a lower $\xi(t, T_{\text{fin}})$ for higher T_{fin} (Figure 4). This observation aligns well

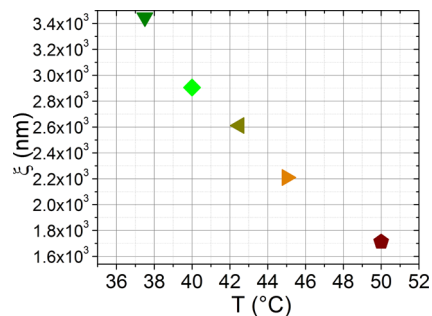


Figure 4. $\xi(t, T_{\text{fin}})$ at long times ($t \approx 870$ s) obtained from the late-stage data of the samples with the highest $\text{HoCl}_3/\text{LaCl}_3$ ratio (cf. Figure 3c).

with a study conducted by Gibaud et al.⁴⁹ on a lysozyme system with an upper critical solution temperature. Gibaud et al. trace back their findings to the fact that arrest occurs in the early stage of spinodal decomposition. Given this explanation and our observation that, in the samples with the highest HoCl_3 concentration, ξ does not grow with time (Figure 3c), we therefore tentatively assume that in this sample arrest can indeed occur at an early stage of phase separation. In addition, the data shown in Figure 4 indicate that even in the arrested state approached at long times for all temperatures in the samples with the highest $\text{HoCl}_3/\text{LaCl}_3$ ratio, $\xi(t, T_{\text{fin}})$ is still tunable by choosing different T_{fin} , which is of potential interest for the fabrication of protein-based materials with temperature-responsive structures.

Considering that both Ho^{3+} and La^{3+} used here are trivalent and part of the lanthanide series, it is remarkable how strong the differences in the kinetics are, induced by only a small change in their relative initial concentrations. Thus, even small changes in the composition of the samples lead to substantial changes in the phase transition kinetics. This is qualitatively consistent with the observation of strong differences in the phase transition temperatures of BSA (cf. Figure 1 and ref 69) upon small changes of the multivalent salt ratios. In the experiments described in ref 69, it was found that Ho^{3+} cations have the strongest affinity to BSA and also induce the strongest BSA–BSA interactions. La^{3+} cations are the weakest agents in both respects. In addition, protein–protein interactions were

found to be fine-tunable by varying cation mixture ratios. These results underline the importance and strength of ion-specific effects also for trivalent ions, similar to the famous Hofmeister series (established mostly for monovalent ions).⁷⁷

By controlling the protein–protein interactions of our systems, we are able to tune the effective depth of the temperature jump^{46,47} into the coexisting regions of our samples by varying the ratio of a salt inducing strong and weak protein–protein interactions (HoCl₃ and LaCl₃, respectively).

Moreover, we are able to influence the onset of arrested states via both strength of the cation-induced protein–protein interaction and temperature. This manifests itself in the increasing deviation from the power law growth of $\xi \sim t^{1/3}$ with increasingly attractive overall interactions. This observation can potentially be explained via the formation of clusters via cation-induced protein bridging.⁶⁶ The fact that arrest occurs at high T_{fin} and at high HoCl₃ concentrations can also be tentatively attributed to the fact that the high protein concentration and the strong interprotein attraction induced by Ho³⁺ cations⁶⁹ can lead to the formation of an attractive glass.³³ Importantly, the present study shows how subtle differences in sample composition, brought about by different salt ratios, can lead to large macroscopic differences in sample behavior and, intriguingly, allow for tuning of the phase behavior in a rational way.

CONCLUSIONS

We have established that the growth of the characteristic length scale $\xi(t, T_{\text{fin}})$ of our systems consisting of BSA with different mixing ratios of trivalent salts slows down with increasing temperature and increasing concentrations of the salt HoCl₃ inducing strongly attractive interactions up to the point that the system appears to be in a locked-in or arrested state. Intriguingly, we are able to influence the onset of arrested states by varying the ratios of different multivalent salts. We note that the specific behavior and the specific differences of (multi)valent ions and in particular their mixtures and interactions with proteins appears to not lend itself to simple explanation. In particular, effects of inhomogeneous cation distribution and their different affinities to proteins^{69,78–80} can play a role. Considering that the Hofmeister series for the seemingly simple monovalent ions was established more than 100 years ago but is still in need of investigation, it is probably not surprising that for the more complex lanthanides a simple explanation appears elusive at present. Nevertheless, the data presented in this publication demonstrate that we can combine two control parameters—temperature and ratio of multivalent salts introducing strong and weak interprotein attraction—to obtain multidimensional control of the phase behavior of the system.

With this paper, we hope to have provided new and interesting data on cation-induced liquid–liquid phase separation and its kinetics in proteins and to stimulate further theoretical work on these highly complex systems. Our results open new opportunities to tune phase transitions not only in proteins but also in colloidal or polymer systems sensitive to external stimuli such as temperature or ionic strength. This is of particular interest for the design and development of smart materials such as gels used to purify water.⁷¹

ASSOCIATED CONTENT

Supporting Information

The Supporting Information is available free of charge on the ACS Publications website at DOI: 10.1021/acs.jpccb.8b10725.

Data set combining USAXS and VSANS data for a sample containing a HoCl₃/LaCl₃ ratio of 22/18 at a T_{fin} of 45 °C (PDF)

AUTHOR INFORMATION

Corresponding Authors

*E-mail: olga.matsarskaia@uni-tuebingen.de (O.M.).

*E-mail: frank.schreiber@uni-tuebingen.de. Phone: +49 (0) 7071 2978670. Fax: +49 (0)7071 295110 (F.S.).

ORCID

Olga Matsarskaia: 0000-0002-7293-7287

Fajun Zhang: 0000-0001-7639-8594

Frank Schreiber: 0000-0003-3659-6718

Present Addresses

#Neutron Scattering Laboratory, Department of Nuclear Physics, China Institute of Atomic Energy, 102413 Beijing, China (Z.F.).

[†]Helmholtz-Institut Ulm für elektrochemische Energiespeicherung, Helmholtzstr. 11, 89081 Ulm, Germany (A.M.).

[‡]EMBL c/o DESY, Notkestr. 85, 22607 Hamburg, Germany (S.D.V.).

Notes

The authors declare no competing financial interest.

ACKNOWLEDGMENTS

The authors gratefully acknowledge the ESRF for beamtime allocation on beamline ID02 and thank the DFG for financial support. O.M. acknowledges a PhD fellowship by the Studienstiftung des Deutschen Volkes and thanks the PSCM (Grenoble) for sharing their laboratory resources as well as A. Girelli and C. Beck for assistance during the USAXS measurements. Helpful discussions with T. Narayanan (ESRF, Grenoble) and R. Roth (Tübingen) are gratefully acknowledged.

REFERENCES

- (1) Baumgart, T.; Hammond, A. T.; Sengupta, P.; Hess, S. T.; Holowka, D. A.; Baird, B. A.; Webb, W. W. Large-scale fluid–fluid phase separation of proteins and lipids in giant plasma membrane vesicles. *Proc. Natl. Acad. Sci. U.S.A.* **2007**, *104*, 3165–3170.
- (2) Berry, J.; Weber, S. C.; Vaidya, N.; Haataja, M.; Brangwynne, C. P. RNA transcription modulates phase transition-driven nuclear body assembly. *Proc. Natl. Acad. Sci. U.S.A.* **2015**, *112*, E5237–E5245.
- (3) Berry, J.; Brangwynne, C. P.; Haataja, M. Physical principles of intracellular organization via active and passive phase transitions. *Rep. Prog. Phys.* **2018**, *81*, No. 046601.
- (4) Lee, C. F.; Brangwynne, C. P.; Hyman, A. A.; Jülicher, F. Spatial Organization of the Cell Cytoplasm by Position-Dependent Phase Separation. *Phys. Rev. Lett.* **2013**, No. 088101.
- (5) Boire, A.; Sanchez, C.; Morel, M.-H.; Lettinga, M. P.; Menut, P. Dynamics of liquid–liquid phase separation of wheat gliadins. *Sci. Rep.* **2018**, *8*, No. 14441.
- (6) Benedek, G. B. Cataract as a protein condensation disease: the Proctor Lecture. *Invest. Ophthalmol. Visual Sci.* **1997**, *38*, 1911–1921.
- (7) Pan, W.; Galkin, O.; Filobelo, L.; Nagel, R. L.; Vekilov, P. G. Metastable Mesoscopic Clusters in Solutions of Sick-Cell Hemoglobin. *Biophys. J.* **2007**, *92*, 267–277.
- (8) Mason, B. D.; van Enk, J. Z.; Zhang, L.; Remmele, R. L., Jr.; Zhang, J. Liquid–Liquid Phase Separation of a Monoclonal Antibody

and Nonmonotonic Influence of Hofmeister Anions. *Biophys. J.* **2010**, *99*, 3792–3800.

(9) Wang, Y.; Wang, Y.; Breed, D. R.; Manoharan, V. N.; Feng, L.; Hollingsworth, A. D.; Weck, M.; Pine, D. J. Colloids with valence and specific directional bonding. *Nature* **2012**, *491*, 51–55.

(10) Raut, A. S.; Kalonia, D. S. Pharmaceutical Perspective on Opalescence and Liquid-Liquid Phase Separation in Protein Solutions. *Mol. Pharmaceutics* **2016**, *13*, 1431–1444.

(11) Mezzenga, R.; Schurtenberger, P.; Burbidge, A.; Michel, M. Understanding foods as soft materials. *Nat. Mater.* **2005**, *4*, 729–740.

(12) Mezzenga, R.; Fischer, P. The self-assembly, aggregation and phase transitions of food protein systems in one, two and three dimensions. *Rep. Prog. Phys.* **2013**, *76*, No. 046601.

(13) ten Wolde, P. R.; Frenkel, D. Enhancement of Protein Crystal Nucleation by Critical Density Fluctuations. *Science* **1997**, *277*, 1975–1978.

(14) Zhang, F.; Zocher, G.; Sauter, A.; Stehle, T.; Schreiber, F. Novel approach to controlled protein crystallization through ligandation of yttrium cations. *J. Appl. Crystallogr.* **2011**, *44*, 755–762.

(15) Schubert, R.; Meyer, A.; Baitan, D.; Dierks, K.; Perbandt, M.; Betzel, C. Real-Time Observation of Protein Dense Liquid Cluster Evolution during Nucleation in Protein Crystallization. *Cryst. Growth Des.* **2017**, *17*, 954–958.

(16) Jones, R. A. L. *Soft Condensed Matter*; Oxford University Press, 2002.

(17) Cahn, J. W.; Hilliard, J. E. Free Energy of a Nonuniform System. III. Nucleation in a Two-Component Incompressible Fluid. *J. Chem. Phys.* **1959**, *31*, 688–699.

(18) Cahn, J. W. Phase separation by spinodal decomposition in isotropic systems. *J. Chem. Phys.* **1965**, *42*, 93–99.

(19) Papon, P.; Schnur, S.; Leblond, J.; Meijer, P. *The Physics of Phase Transitions: Concepts and Applications*; Advanced Texts in Physics; Springer: Berlin, 2006.

(20) Lifshitz, I. M.; Slyozov, V. The kinetics of precipitation from supersaturated solid solutions. *J. Phys. Chem. Solids* **1961**, *19*, 35–50.

(21) Huse, D. A. Corrections to late-stage behavior in spinodal decomposition: Lifshitz-Slyozov scaling and Monte Carlo simulations. *Phys. Rev. B* **1986**, *34*, No. 7845.

(22) Binder, K.; Stauffer, D. Theory for the slowing down of the relaxation and spinodal decomposition of binary mixtures. *Phys. Rev. Lett.* **1974**, *33*, No. 1006.

(23) Rundman, K.; Hilliard, J. Early stages of spinodal decomposition in an aluminum-zinc alloy. *Acta Metall.* **1967**, *15*, 1025–1033.

(24) Laughlin, D.; Cahn, J. W. Spinodal decomposition in age hardening copper-titanium alloys. *Acta Metall.* **1975**, *23*, 329–339.

(25) Bruder, F.; Brenn, R. Spinodal Decomposition in Thin Films of a Polymer Blend. *Phys. Rev. Lett.* **1992**, *69*, No. 624.

(26) Bates, F. S.; Wiltzius, P. Spinodal decomposition of a symmetric critical mixture of deuterated and protonated polymer. *J. Chem. Phys.* **1989**, *91*, 3258–3274.

(27) Ramírez-Santiago, G.; González, A. E. Growth laws and spinodal decomposition type of scaling in fractal aggregation of colloids. *Phys. A* **1997**, *236*, 75–84.

(28) Sedgwick, H.; Kroy, K.; Salonen, A.; Robertson, M.; Egelhaaf, S.; Poon, W. Non-equilibrium behavior of sticky colloidal particles: beads, clusters and gels. *Eur. Phys. J. E* **2005**, *16*, 77–80.

(29) Lu, P. J.; Zaccarelli, E.; Ciulla, F.; Schofield, A. B.; Sciortino, F.; Weitz, D. A. Gelation of particles with short-range attraction. *Nature* **2008**, *453*, 499–503.

(30) Verhaegh, N. A.; van Duijneveldt, J. S.; Dhont, J. K.; Lekkerkerker, H. N. Fluid-fluid phase separation in colloid-polymer mixtures studied with small angle light scattering and light microscopy. *Phys. A* **1996**, *230*, 409–436.

(31) Dhont, J. K. G. *An Introduction to Dynamics of Colloids*; Elsevier Science B. V., 1996.

(32) Dhont, J. K. G. Spinodal decomposition of colloids in the initial and intermediate stages. *J. Chem. Phys.* **1996**, *105*, S122–S125.

(33) Zaccarelli, E. Colloidal gels: equilibrium and non-equilibrium routes. *J. Phys.: Condens. Matter* **2007**, *19*, No. 323101.

(34) Sperry, P. R.; Hopfenberg, H. B.; Thomas, N. L. Flocculation of latex by water-soluble polymers: Experimental confirmation of a nonbridging, nonadsorptive, volume-restriction mechanism. *J. Colloid Interface Sci.* **1981**, *82*, 62–76.

(35) Gast, A. P.; Hall, C. K.; Russel, W. B. Phase Separations Induced in Aqueous Colloidal Suspensions by Dissolved Polymer. *Faraday Discuss. Chem. Soc.* **1983**, *76*, 189–201.

(36) Gast, A. P.; Russel, W. B.; Hall, C. K. An Experimental and Theoretical Study of Phase Transitions in the Polystyrene Latex and Hydroxyethylcellulose System. *J. Colloid Interface Sci.* **1986**, *109*, 161–171.

(37) Hagen, M. H. J.; Frenkel, D. Determination of phase diagrams for the hard-core attractive Yukawa system. *J. Chem. Phys.* **1994**, *101*, 4093–4097.

(38) Lomba, E.; Almarza, N. G. Role of the interaction range in the shaping of phase diagrams in simple fluids. The hard sphere Yukawa fluid as a case study. *J. Chem. Phys.* **1994**, *100*, 8367–8372.

(39) Anderson, V. J.; Lekkerkerker, H. N. W. Insights into phase transition kinetics from colloid science. *Nature* **2002**, *416*, 811–815.

(40) Ishimoto, C.; Tanaka, T. Critical Behavior of a Binary Mixture of Protein and Salt Water. *Phys. Rev. Lett.* **1977**, *39*, 474–477.

(41) Thomson, J. A.; Schurtenberger, P.; Thurston, G. M.; Benedek, G. B. Binary liquid phase separation and critical phenomena in a protein/water solution. *Proc. Natl. Acad. Sci. U.S.A.* **1987**, *84*, 7079–7083.

(42) Broide, M. L.; Berland, C. R.; Pande, J.; Ogun, O. O.; Benedek, G. B. Binary-liquid phase separation of lens protein solutions. *Proc. Natl. Acad. Sci. U.S.A.* **1991**, *88*, 5660–5664.

(43) Muschol, M.; Rosenberger, F. Liquid-liquid phase separation in supersaturated lysozyme solutions and associated precipitate formation/crystallization. *J. Chem. Phys.* **1997**, *107*, 1953–1962.

(44) Galkin, O.; Chen, K.; Nagel, R. L.; Hirsch, R. E.; Vekilov, P. G. Liquid-liquid separation in solutions of normal and sickle cell hemoglobin. *Proc. Natl. Acad. Sci. U.S.A.* **2002**, *99*, 8479–8483.

(45) Annunziata, O.; Ogun, O.; Benedek, G. B. Observation of liquid-liquid phase separation for eye lens γ S-crystallin. *Proc. Natl. Acad. Sci. U.S.A.* **2003**, *100*, 970–974.

(46) Shah, M.; Galkin, O.; Vekilov, P. G. Smooth transition from metastability to instability in phase separating protein solutions. *J. Chem. Phys.* **2004**, *121*, 7505–7512.

(47) Cardinaux, F.; Gibaud, T.; Stradner, A.; Schurtenberger, P. Interplay between Spinodal Decomposition and Glass Formation in Proteins Exhibiting Short-Range Attractions. *Phys. Rev. Lett.* **2007**, *99*, No. 118301.

(48) Gliko, O.; Pan, W.; Katsonis, P.; Neumaier, N.; Galkin, O.; Weinkauff, S.; Vekilov, P. G. Metastable Liquid Clusters in Super- and Undersaturated Protein Solutions. *J. Phys. Chem. B* **2007**, *111*, 3106–3114.

(49) Gibaud, T.; Schurtenberger, P. A closer look at arrested spinodal decomposition in protein solutions. *J. Phys.: Condens. Matter* **2009**, *21*, No. 322201.

(50) Wang, Y.; Lomakin, A.; Latypov, R. F.; Benedek, G. B. Phase separation in solutions of monoclonal antibodies and the effect of human serum albumin. *Proc. Natl. Acad. Sci. U.S.A.* **2011**, *108*, 16606–16611.

(51) Zhang, F.; Skoda, M. W. A.; Jacobs, R. M. J.; Zorn, S.; Martin, R. A.; Martin, C. M.; Clark, G. F.; Weggler, S.; Hildebrandt, A.; Kohlbacher, O.; Schreiber, F. Reentrant Condensation of Proteins in Solution Induced by Multivalent Counterions. *Phys. Rev. Lett.* **2008**, *101*, No. 148101.

(52) Zhang, F.; Weggler, S.; Ziller, M. J.; Ianeselli, L.; Heck, B. S.; Hildebrandt, A.; Kohlbacher, O.; Skoda, M. W. A.; Jacobs, R. M. J.; Schreiber, F. Universality of protein reentrant condensation in solution induced by multivalent metal ions. *Proteins* **2010**, *78*, 3450–3457.

(53) Zhang, F.; Roth, R.; Wolf, M.; Roosen-Runge, F.; Skoda, M. W. A.; Jacobs, R. M. J.; Sztucki, M.; Schreiber, F. Charge-controlled

metastable liquid-liquid phase separation in protein solutions as a universal pathway towards crystallization. *Soft Matter* **2012**, *8*, 1313–1316.

(54) Roosen-Runge, F.; Heck, B. S.; Zhang, F.; Kohlbacher, O.; Schreiber, F. Interplay of pH and Binding of Multivalent Metal Ions: Charge Inversion and Reentrant Condensation in Protein Solutions. *J. Phys. Chem. B* **2013**, *117*, 5777–5787.

(55) Zhang, F.; Roosen-Runge, F.; Sauter, A.; Roth, R.; Skoda, M. W. A.; Jacobs, R.; Sztucki, M.; Schreiber, F. The Role of Cluster Formation and Metastable Liquid-Liquid Phase Separation in Protein Crystallization. *Faraday Discuss.* **2012**, *159*, 313–325.

(56) Zhang, F.; Roosen-Runge, F.; Sauter, A.; Wolf, M.; Jacobs, R. M. J.; Schreiber, F. Reentrant Condensation, Liquid-Liquid Phase Separation and Crystallization in Protein Solutions Induced by Multivalent Metal Ions. *Pure Appl. Chem.* **2014**, *86*, 191–202.

(57) Wolf, M.; Roosen-Runge, F.; Zhang, F.; Roth, R.; Skoda, M. W.; Jacobs, R. M.; Sztucki, M.; Schreiber, F. Effective interactions in protein-salt solutions approaching liquid-liquid phase separation. *J. Mol. Liq.* **2014**, *200*, 20–27.

(58) Sauter, A.; Oelker, M.; Zocher, G.; Zhang, F.; Stehle, T.; Schreiber, F. Nonclassical Pathways of Protein Crystallization in the Presence of Multivalent Metal Ions. *Cryst. Growth Des.* **2014**, *14*, 6357–6366.

(59) Sauter, A.; Roosen-Runge, F.; Zhang, F.; Lotze, G.; Jacobs, R. M. J.; Schreiber, F. Real-Time Observation of Nonclassical Protein Crystallization Kinetics. *J. Am. Chem. Soc.* **2015**, *137*, 1485–1491.

(60) Sauter, A.; Roosen-Runge, F.; Zhang, F.; Lotze, G.; Feoktystov, A.; Jacobs, R. M. J.; Schreiber, F. On the question of two-step nucleation in protein crystallization. *Faraday Discuss.* **2015**, *179*, 41–58.

(61) Sauter, A.; Zhang, F.; Szekely, N. K.; Pipich, V.; Sztucki, M.; Schreiber, F. Structural Evolution of Metastable Protein Aggregates in the Presence of Trivalent Salt Studied by (V)SANS and SAXS. *J. Phys. Chem. B* **2016**, *120*, 5564–5571.

(62) Matsarskaia, O.; Braun, M. K.; Roosen-Runge, F.; Wolf, M.; Zhang, F.; Roth, R.; Schreiber, F. Cation-induced Hydration Effects Cause Lower Critical Solution Temperature Behavior in Protein Solutions. *J. Phys. Chem. B* **2016**, *120*, 7731–7736.

(63) Braun, M. K.; Wolf, M.; Matsarskaia, O.; da Vela, S.; Roosen-Runge, F.; Sztucki, M.; Roth, R.; Zhang, F.; Schreiber, F. Strong Isotope Effects on Effective Interactions and Phase Behavior in Protein Solutions in the Presence of Multivalent Ions. *J. Phys. Chem. B* **2017**, *121*, 1731–1739.

(64) Da Vela, S.; Braun, M. K.; Dörr, A.; Greco, A.; Möller, J.; Fu, Z.; Zhang, F.; Schreiber, F. Kinetics of liquid-liquid phase separation in protein solutions exhibiting LCST phase behavior studied by time-resolved USAXS and VSANS. *Soft Matter* **2016**, *12*, 9334–9341.

(65) Fries, M. R.; Stopper, D.; Braun, M. K.; Hinderhofer, A.; Zhang, F.; Jacobs, R. M. J.; Skoda, M. W. A.; Hansen-Goos, H.; Roth, R.; Schreiber, F. Multivalent-ion-activated protein adsorption reflecting bulk reentrant behavior. *Phys. Rev. Lett.* **2017**, *119*, No. 228001.

(66) Roosen-Runge, F.; Zhang, F.; Schreiber, F.; Roth, R. Ion-activated Attractive Patches as a Mechanism for Controlled Protein Interactions. *Sci. Rep.* **2014**, *4*, No. 7016.

(67) Bianchi, E.; Capone, B.; Coluzza, I.; Rovigatti, L.; van Oostrum, P. D. J. Limiting the valence: advancements and new perspectives on patchy colloids, soft functionalized nanoparticles and biomolecules. *Phys. Chem. Chem. Phys.* **2017**, *19*, 19847–19868.

(68) Sudlow, G.; Birkett, D. J.; Wade, D. N. Spectroscopic techniques in the study of protein binding. A fluorescence technique for the evaluation of the albumin binding and displacement of warfarin and warfarin-alcohol. *Clin Exp Pharmacol Physiol.* **1975**, *2*, 129–140.

(69) Matsarskaia, O.; Roosen-Runge, F.; Lotze, G.; Möller, J.; Mariani, A.; Zhang, F.; Schreiber, F. Tuning phase transitions of aqueous protein solutions by multivalent cations. *Phys. Chem. Chem. Phys.* **2018**, *20*, 27214–27225.

(70) Da Vela, S.; Exner, C.; Schäufele, R. S.; Möller, J.; Fu, Z.; Zhang, F.; Schreiber, F. Arrested and temporarily arrested states in a protein-polymer mixture studied by USAXS and VSANS. *Soft Matter* **2017**, *13*, 8756–8765.

(71) Okesola, B. O.; Smith, D. K. Applying low-molecular weight supramolecular gelators in an environmental setting self-assembled gels as smart materials for pollutant removal. *Chem. Soc. Rev.* **2016**, *45*, 4226–4251.

(72) Constantin, M.; et al. Lower critical solution temperature versus volume phase transition temperature in thermoresponsive drug delivery systems. *Express Polym. Lett.* **2011**, *5*, 839–848.

(73) Lehninger, A. L.; Nelson, D. L.; Cox, M. M. *Lehninger Principles of Biochemistry*; W. H. Freeman: New York, 2005.

(74) Van Vaerenbergh, P.; Léonardon, J.; Sztucki, M.; Boesecke, P.; Gorini, J.; Claustre, L.; Sever, F.; Morse, J.; Narayanan, T. In *An Upgrade Beamline for Combined Wide, Small and Ultra Small-Angle X-ray Scattering at the ESRF*, AIP Conference Proceedings, 2016; p 030034.

(75) Narayanan, T.; Sztucki, M.; van Vaerenbergh, P.; Léonardon, J.; Gorini, J.; Claustre, L.; Sever, F.; Morse, J.; Boesecke, P. A multipurpose instrument for time-resolved ultra small-angle and coherent X-ray scattering. *J. Appl. Crystallogr.* **2018**, *51*, 1511–1524.

(76) Pipich, V.; Fu, Z. KWS-3: Very small angle scattering diffractometer with focusing mirror. *J. Large-Scale Res. Facil.* **2015**, *1*, 31.

(77) Okur, H. I.; Hladílková, J.; Rembert, K. B.; Cho, Y.; Heyda, J.; Dzubiel, J.; Cremer, P. S.; Jungwirth, P. Beyond the Hofmeister Series: Ion-Specific Effects on Proteins and Their Biological Functions. *J. Phys. Chem. B* **2017**, *121*, 1997–2014.

(78) Schomäcker, K.; Mocker, D.; Münze, R.; Beyer, G.-J. Stabilities of lanthanide-protein complexes. *Int. J. Rad. Appl. Instrum. A Appl. Radiat. Isot.* **1988**, *39*, 261–264.

(79) Smolka, G. E.; Birnbaum, E. R.; Darnall, D. W. Rare earth metal ions as substitutes for the calcium ion in *Bacillus subtilis* alpha-amylase. *Biochemistry* **1971**, *10*, 4556–4561.

(80) Gomez, J. E.; Birnbaum, E. R.; Darnall, D. W. Metal ion acceleration of the conversion of trypsinogen to Trypsin. Lanthanide ions as calcium ion substitutes. *Biochemistry* **1974**, *13*, 3745–3750.